Influence of the nature of aggregates on the behaviour of concrete subjected to elevated temperature

Zhi Xing [a], Anne-Lise Beaucour [a,*], Ronan Hebert [b], Albert Noumowe [a], Béatrice Ledesert [b]

[a] Université de Cergy-Pontoise, L2MGC, EA 4114, F-95000 Cergy-Pontoise, France
[b] Université de Cergy-Pontoise, Géosciences et Environnement Cergy, EA 4506, F-95000 Cergy-Pontoise, France

ARTICLE INFO

ABSTRACT

An experimental study is carried out on concretes composed of three different types of aggregates: semi crushed silico-calcareous, crushed calcareous and rolled siliceous. For each aggregate type, two water/cement ratios (W/C), 0.6 and 0.3 are studied. Aggregates and concrete specimens were subjected to 300, 600 and 750 °C heating–cooling cycles. We analyse the evolution of thermal, physical and mechanical properties of concrete in terms of behaviour and physical characteristic evolutions of aggregates with temperature. The study of thermal behaviour of aggregates showed the importance of initial moisture state for the flints. The crystallisation and microstructure of quartz play an important role in the thermal stability of siliceous aggregates. The residual mechanical behaviour of concrete varies depending on the aggregate and the influence of aggregates is also dependent on paste composition. This study allowed to better understand the influence of chemical and mineralogical characteristics of aggregates on the thermomechanical behaviour of concrete.

© 2011 Elsevier Ltd. All rights reserved.

1. Introduction

The high temperature concrete behaviour is strongly linked to the properties of the cement paste. Indeed, it is within the cement paste that occur the main phenomena of dehydration and expulsion of moisture that lead to concrete deterioration. For about fifteen years, several studies have improved the understanding of the physico-chemical and microstructural evolution of the binding phase [1–4]. But does it mean that aggregates only play a negligible role? Aggregates represent a considerable proportion of volume in the concrete and the thermal conductivity of concrete must be considerably influenced by the thermal conductivity of aggregates. In addition, according to their mineralogical composition and their internal microstructure, it is very likely that aggregates have very different values of thermal conductivities. Moreover, this conductivity evolves differently with temperature depending on the type of aggregates. On the other hand, because of bleeding and a wall effect, there is an accumulation of water at the paste–aggregate interface. This greater water quantity creates a more porous zone in which cracking will be initiated. The aggregate-matrix interface can therefore be considered as the "weak link" of ordinary concrete and is often causing the concrete deterioration. The quality of the paste–aggregate bond is highly dependent on the geometry of the aggregates and on their mineralogical nature (reactive or not with the paste) [5,6].

Then it appears necessary to complete the existing studies about the influence of aggregates on the thermomechanical behaviour of concrete.

Few studies have been published until now [7–11]. Several studies showed that a concrete made of siliceous aggregate has worse behaviour than a calcareous aggregate concrete [8,10,12]. The decrease in compressive strength of calcareous aggregate concretes occurs at higher temperatures compared to siliceous aggregate concretes [13]. This is generally attributed to the higher thermal expansion of siliceous aggregates and to the volume increase due to the phase transition (at 573 °C) from α-quartz to β-quartz [14,15]. Some authors also explain that the specific heat of calcareous aggregates is higher than that of siliceous aggregates and that the specific heat of calcareous aggregates is approximately ten times the heat needed to produce the same temperature rise in siliceous aggregates over 600 °C[16]. So carbonate aggregates may increase the fire endurance of concrete compared to that of siliceous aggregates [16,17]. Nevertheless, [11] showed that concretes prepared with some siliceous aggregates can have better mechanical residual behaviour than those with calcareous aggregates. The results of this study disagree with the Eurocode 2-1-2 predictions [12]. Moreover, the carbonates, which have broken down releasing carbon dioxide during heating, re-hydrate during cooling. This re-hydration reaction (44% increases in volume) is believed to cause "post-cooling spalling" in calcareous concretes [18]. These information show that previous studies need to be completed by experimental data on the thermomechanical behaviour of concretes prepared with different natures of aggregates in order to provide a better understanding of the influence of the chemical composition and mineralogy of aggregates.

The objective of this study is to analyse the influence of aggregates on the high temperature behaviour of normal and high performance concretes. Three different types of aggregates are studied (see below for details). Aggregates were subjected to 5 individual heating–cooling cycles

---

* Corresponding author. Tel.: +33 1 34 25 69 75; fax: +33 1 34 25 69 41.
E-mail address: Anne-Lise.Beaucour@u-cergy.fr (A.-L. Beaucour).

at 150 °C, 300 °C, 450 °C, 600 °C and 750 °C at a heating rate of 1 °C/min. The evolution of aggregate characteristics like temperature, mass loss, porosity, thermal stability is analysed. Ordinary concretes and high-performance concretes are made with each of the three types of aggregates. The concrete specimens, as well as the aggregates on their own undergo the same thermal scenario but just for 300 °C, 600 °C and 750 °C.

The mechanical behaviour of concrete can be studied during the heating (fire) or during a post-fire situation (residual behaviour). In this paper the study focuses on post-fire (residual) behaviour. Such data are useful in situations when redesign of fire-damaged concrete elements is considered and in assessing the durability of concrete structures after the fire. During the cooling process, the thermal induced stress is opposite which can cause severe cracks [4,19]. Furthermore, the free CaO can react with the ambient relative humidity and be transformed into Ca(OH)$_2$. This reaction which also corresponds to a volume increase ($x2$) generates cracking and crumbling of concrete. The experience shows that the "hot" concrete specimens exhibit greater compressive strength and Young modulus than the "residual" concrete after cooling [13,20–24].

The residual mechanical properties and thermal and physical characteristics of concrete are measured after cooling. Decreases in mechanical performance of concretes following the temperature rise are analysed in terms of physico-chemical properties and thermal properties of aggregates. The effect of aggregate type is also analysed with respect to matrix quality (water/cement ratio, W/C). The results provide elements to understand the influence of aggregates on the thermomechanical behaviour of concrete.

2. Experimental campaign

2.1. Aggregates

Three different types of aggregates are used in the experiments: semi-crushed silico-calcareous aggregates extracted from Seine River (6.3/20 mm), rolled siliceous aggregates (2/14 mm and 14/20 mm) and crushed calcareous aggregates (6.3/14 mm and14/20 mm). The densities of these three types of aggregates measured in the laboratory according to standard EN 1097-6 are 2482, 2592 and 2670 kg/m^3, respectively. The sands used have the same composition as the aggregates and come from the same sources. Their granular class and density are 0/4 mm, 2458 kg/m^3 for the silico-calcareous aggregates, 0/2 mm, 2563 kg/m^3 for the siliceous rolled aggregates and 0/4, 2686 kg/m^3 for the calcareous aggregates that contain approximately 15% of siliceous elements.

Using a quartage method [25], a representative sample of about 5 kg of each type of aggregates is obtained from an initial stock of 500 kg. The

different aggregates are analysed by macroscopic observation with a magnifying lens and by using a hydrochloric acid solution to react with the carbonates. The different natures of rocks constituting the aggregates are separated and identified at this step. The respective proportions of the different groups are estimated in Table 1 and petrographic composition of the aggregates is determined.

The calcareous (C) aggregates consist of nearly pure carbonate, forming a homogeneous population. The silico-calcareous (SC) aggregates present a large petrographic variety. It is mainly composed of flint (70%), carbonate (24%) and silica-rich rocks of different compositions and origins (sandstone, quartzite, microconglomerate, granite, etc.). The siliceous (S) aggregates contain quartzite (91%), sandstone (7%) and other rock types (2%) as flint, micro-conglomerate, schist, carbonate rock, etc. A complete petrographic description of the 3 aggregates types is provided in Table 1.

The C aggregates are angular and irregular in shape. The surface of the particles is smooth with uniform colour.

Among the SC aggregates, the shape of flint particles is angular, rounded or irregular. Their surface texture is smooth. Some flint particles are partly wrapped in a cortex. The shape of carbonate particles is flattened, elongated and irregular. Their surface texture is rough. Some carbonates have a microporous surface. Sandstone pebbles have an irregular shape and their colours are white or reddish. Quartzite particles of SC aggregates have rounded shape and are composed of many crystals of white translucent grains of quartz.

The quartzite particles of the S aggregates have a rounded shape and a smooth surface texture. The sandstone particles have a rounded or flattened shape and a rough surface texture.

The shape and surface texture of aggregates will affect the quality of the paste/aggregate interface. It can be expected that cracking or debounding at the interface as a result of differential thermal expansion between the aggregates and the cement paste can be limited or delayed for angular and rough aggregates compared to rounded and smooth aggregates.

2.2. Compositions of concretes

For each of the three types of aggregates, two types of formulation are studied, a normal concrete (NC) with a W/C of 0.6 and a high-performance concrete (HPC) with a W/C of 0.3. Compositions of concretes are listed in Table 2. Portland cement (CEMI 52.5) is used. The dosage of superplasticizer (modified polycarboxylate) is adjusted to maintain a constant workability, very plastic (S4) for all the compositions.

Cylindrical specimens (Ø16×32 cm and Ø11×22 cm) are prepared. After seven days, the specimens are demoulded and placed into sealed plastic bags at ambient temperature for 90 days in accordance with the curing conditions of the RILEM recommendations [26].

Table 1
Petrographic composition of calcareous, silico-calcareous and siliceous aggregates (values are expressed in wt.%).

Calcareous (C)		Silico-calcareous (SC)		Siliceous (S)	
Carbonate rock	99.5%	Flint	70%	Quartzite	91%
➢ Dark grey carbonate	58%	➢ Black flint	10%	➢ White quartzite	28%
➢ Dark brown carbonate	27%	➢ Grey flint	17%	➢ Brown quartzite	28%
➢ Light brown carbonate	6.5%	➢ Brown flint	36%	➢ Light grey quartzite	23%
➢ Light grey carbonate	4%	➢ Beige flint	7%	➢ Dark grey quartzite	10%
➢ Red carbonate	1%	Carbonate rock	24%	➢ Various	2%
➢ Multi-phase carbonate	1.5%	➢ White carbonate	12%	Sandstone	7%
➢ Calcite and carbonate rock	1.5%	➢ Brown carbonate	7%	➢ Grey sandstone	4%
➢ Pure Calcite	Accessory	➢ Grey carbonate	5%	➢ Light sandstone	1%
Flint	Accessory	Sandstone	5%	➢ Brown sandstone	2%
Sandstone	Accessory	Quartzite	0.5%	Flint	1%
Iron oolithe	Accessory	Micro-conglomerate	Accessory	Micro-conglomerate	Accessory
		Granite	Accessory	Schiste	Accessory
		Rhyolite	Accessory	Carbonate rock	Accessory
		Basalte	Accessory	Magmatique rock	Accessory
				Siltite	Accessory

Table 2
Mixture of proportions, compressive strength, and elastic modulus of the tested concretes.

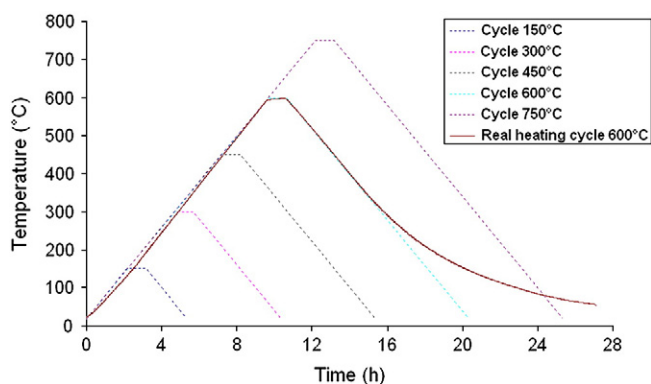|	NC-SC	NC-C	NC-S	HPC-SC	HPC-C	HPC-S
Mineralogical nature	Silico-calcareous	Calcareous	Siliceous	Silico-calcareous	Calcareous	Siliceous
Cement CEM I 52.5 [kg/m³]	362	362	362	500	500	500
Coarse aggregates [kg/m³]	956	447	396	987	459	411
Fine aggregates [kg/m³]		625	740		646	764
Sand [kg/m³]	692	714	585	715	738	604
Water [kg/m³]	217	217	217	150	150	150
Superplasticizer [kg/m³]				1.65	2.15	1.5
[% by mass of cement]				0.33%	0.43%	0.30%
W/C	0.6	0.6	0.6	0.3	0.3	0.3
Volumic mass [kg/m³]	2227	2365	2300	2354	2495	2431
Compressive strength (MPa) before heating	35.9	38.1	38.8	81.2	76.3	72.8
Tensile strength (MPa) before heating	3.7	3.2	4	5.2	4.6	5.9
Young's modulus (GPa) before heating	35.6	31.5	36.6	45.2	43.4	44.2

2.3. Heating/cooling cycles

2.3.1. Heating/cooling methodology

The aggregates and concrete specimens were separately subjected to five independent heating/cooling cycles with maximum temperatures fixed at 150 °C, 300 °C, 450 °C, 600 °C and 750 °C. Each cycle consists of 3 phases: heating-up at a rate of 1 °C/min, stabilisation at constant temperature during one hour and finally cooling to the ambient temperature. This rate is used so that the thermal gradient inside the sample will not be sufficient to create high internal stresses. Fig. 1 shows the theoretical evolution of temperature as a function of time for the five temperature cycles. The real evolution of temperature obtained with a heating up to 600 °C is also indicated. We observe that the real temperature is very close to the theoretical evolution during heating, whereas the cooling is slower which reduces the risk of thermal shock.

In order to investigate the influence of initial moisture content, aggregates are tested saturated and oven-dried before heating. For saturated state, aggregates are immersed in water for 24 h. Water absorption after 24 h becomes very low. For dry state, aggregates are dried at 105 °C until weights of individual grain varied no more than 0.01 g on succeeding days. Their cooling takes place in a desiccator after exit from the oven.

2.3.2. Heating/cooling device

The heating/cooling cycles are performed in a programmable oven with size of $1.3 \times 1.1 \times 1.04$ m. This oven allows to heat large specimens up to 1000 °C. The temperature rise is controlled by a regulator-controller connected to a thermocouple in the oven. A ventilator associated with the heating can regulate and homogenise the temperature by the air circulation between the heating elements. Thermocouples are used to monitor temperature at the upper surface and inside the concrete specimen (this last thermocouple is set up right at the centre of the sample). The thermocouples of type K are connected to an automatic data acquisition system HP323 which records and transmits to the computer the values of temperature versus time. It is the surface temperature of concrete which controls the temperature rise of the oven. Thermocouples of type K placed on three different concrete specimens allow ensuring of the temperature homogeneity in the oven (Fig. 2).

For each mix and each temperature cycle, ten specimens of concretes were stored in the oven. Each batch was composed of four cylindrical specimens Ø16 × 32 cm, three cylindrical specimens Ø11 × 22 cm for the mechanical tests and two cylindrical specimens Ø11 × 11 cm for the thermal conductivity tests and one cylindrical specimen Ø16 × 5 cm for the cracking study. All the specimens were stored in the oven in the same condition in order to have a uniform temperature. Fig. 2 shows the layout of the oven with the concrete specimens.

2.4. Tests

2.4.1. Water porosity

The water porosity of aggregates was measured according to the European standards EN 1936. The volume of voids is deduced from the mass difference between the dry state and the saturated surface-dry condition. The dry mass of aggregates (Ms) is obtained after drying in an oven at 60 °C to constant mass. Aggregates are vacuum saturated and then immersed for 24 h. They were weighed after surface drying (Mw). The apparent volume of aggregates is measured by hydrostatic weighing of saturated aggregates (M'w). The porosity (n) is calculated from the following formula: $n = 100 (Mw - Ms)/(Mw - M'w)$.

2.4.2. Thermal conductivity

The thermal conductivity of concretes, at room temperature, is measured with a Hot-Disk probe TPS1500. The system is based on the technology of the Transient Plane Source (TPS). This method has been developed at Chalmers University of Technology by Gustafsson [27]. A sensor chosen with radius 9.868 mm consisting of a very fine nickel double-spiral (thickness 10 μm) covered with two thin layers of electrically-insulating material is placed between two symmetrical cylinders of concrete Ø11 × 11 cm samples. The two sample pieces are

Fig. 1. Thermal profiles of the different heating–cooling cycles.
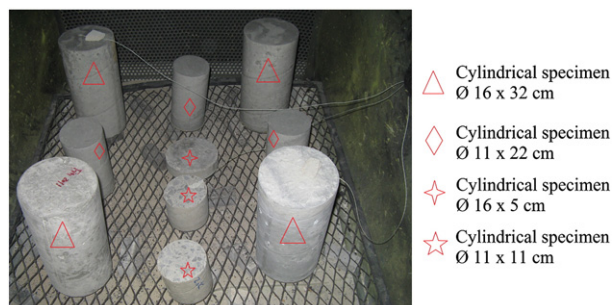
Fig. 2. Layout of the concrete specimens in the oven.

prepared with a section of flat surface each in order to obtain a contact surface with the thinner air layer as possible. During measurement, an electric current passes through the probe and creates an increase of temperature. The heat generated dissipates through the sample on both sides at a rate that depends on the thermal transport characteristics of the material. By recording the temperature versus time response in the sensor, thermal conductivity is calculated [28]. The probe constitutes both heat source and temperature sensor. The conductivity measurement is performed 5 times for each sample. At each measurement, the probe is moved in order to consider the concrete heterogeneity. The mean standard deviation of each set of measurements at 20 °C is 5%, 11% and 9% for thermal conductivity, thermal diffusivity and specific heat respectively. The mean value obtained by moving the sensor is representative of the entire sample. However for samples heated at 750 °C, significant cracking decreases the accuracy of the measurement. Error bars showing the standard deviation of the respective measurements are included in the graph of the evolution of thermal conductivity versus heating temperature (Fig. 8) to point out the significance of the results. In the Hot Disk Analysis v5.9 software the values of parameters "Output of Power" and "Measuring Time" (0.3 W and 40 s, respectively) are chosen in order to optimise the settings of experiment. The five measurements are taken at one hour interval in order to prevent heat generated by current flow in the disc which disturbs the thermal field of the specimen [29].

2.4.3. Mechanical tests

2.4.3.1. Compression tests.
Uniaxial compression tests are performed by using a hydraulic press SCHENCK 3000kN according to standard EN 12390-3. Axial displacements of the specimens are measured in its median part during the test by three displacement transducers LVDT supported by aluminium rings in contact with the specimen. The specimens undergo three loading–unloading cycles from 0.5 MPa to the third of the ultimate load. The first cycle is to avoid measurements affected by plastic deformations. The Young's modulus is then determined from the slopes of the second and third cycle according to the procedure recommended by LCPC [30]. The values of Young's modulus and of compressive strength result from an average performed on 3 specimens. These tests are conducted for each formulation and each heating/cooling cycle.

2.4.3.2. Tension tests.
The tensile strength of concrete is measured by splitting on specimens Ø11×22 cm according to standard EN 12390-6. These tests are performed on three samples, after cooling, for each formulation and each heating cycle.

3. Results and discussion

3.1. Evolution of the characteristics of the different aggregates with temperature

3.1.1. Visual observations
C aggregates: The carbonates remain intact up to 600 °C for initially saturated or dried before heating. At 600 °C, we can observe a colour change for some aggregates, becoming gradually more reddish. At 750 °C, they are cracked and the grain surface has whitened. This is due to the decarbonation: a proportion of calcite ($CaCO_3$) is converted into lime CaO releasing CO_2. About three days after leaving the sample at room temperature, aggregates disintegrate (Fig. 3). After cooling, the free CaO reacts with ambient relative humidity and is transformed into $Ca(OH)_2$ (portlandite) with a volume expansion of 200% [31].

SC aggregates (Fig. 4): in the case of saturated grains, some black flints have burst between 150 and 300 °C. At 450 °C, most of the flints, whatever their colour, have exploded. All of the flints showed cracks. This instability of flint has also been observed in other works [32–34]. The colour of the brown flints has turned into red at 300 °C. The core of all the flints began to bleach from 600 °C. At 750 °C, the bleaching has reached all of the flint
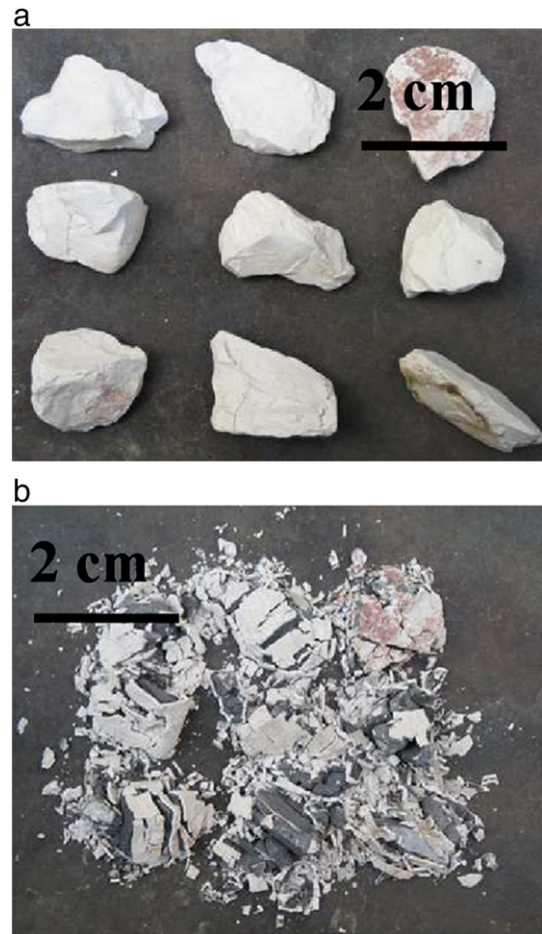
Fig. 3. Comparison of calcareous aggregates before and after transformation from CaO to Portlandite after heating at 750 °C, (a) immediately after heating–cooling cycle at 750 °C, and (b) 3 days after heating–cooling cycle at 750 °C.

grains except the brown flints which remain red. In the case of dry grains, most of the flints have exploded between 450 and 600 °C, whatever their colour and all of them were cracked. Carbonates of SC aggregates appear intact up to 600 °C but cracked at 750 °C. The quartzites remain intact up to 750 °C except a slight and gradual reddening of colour that is observed at 600 °C. Sandstone, granite and rhyolite do not show any transformation up to 750 °C.

S aggregates: The quartzites and the sandstones remain intact up to 750 °C. Slight and gradual reddening appears from 600 °C.

The initial moisture condition seems to have a major influence on the thermal stability of flints. Permeability of flints would be insufficient for allowing water vapour to be evacuated. The vapour pressure in pores increases with the temperature and may cause the spalling of saturated flints between 150 °C and 450 °C. The explosive behaviour of initially dried flints between 450 °C and 600 °C could be also explained by an excessive pressure of water vapour. Flint can contain hydrated silica: water molecules in micropores or silanol groups ($SiO_{5/2}$ H) [35]. The amount of this trapped water is estimated at about 1% [36]. During the heating, the silanol groups are condensed to give lose water [37,38]. Other authors assumed that the presence of calcite or iron oxides into the flints could explain their thermal damage [39–41].

3.1.2. Aggregate porosity
For each of the three types of aggregates, 15 grains of each lithologic nature are tested. An average porosity for each lithologic type is calculated from measurements made on these 15 grains. The overall porosity of an
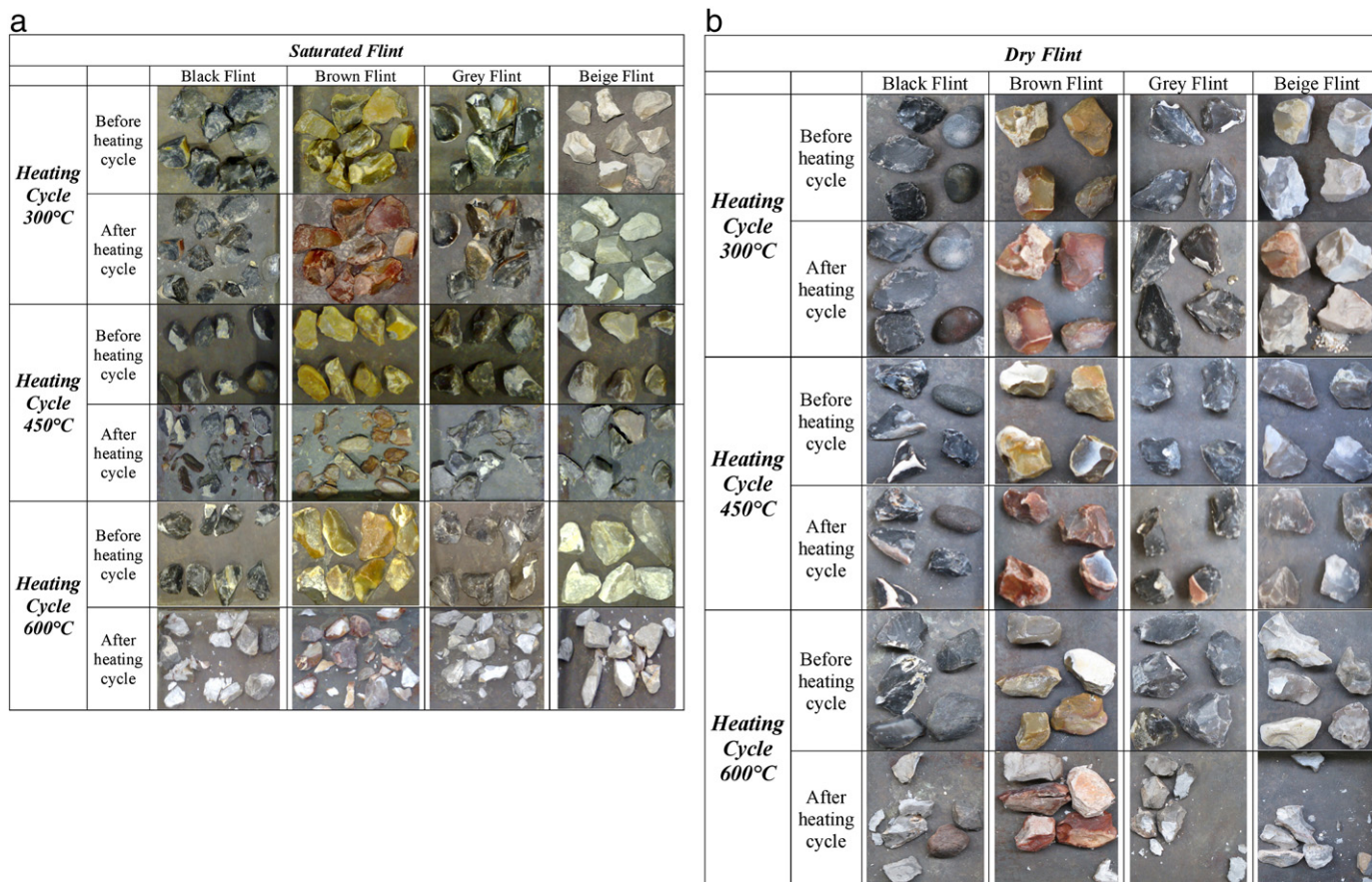
a

b

Fig. 4. Comparison of different types of flint before and after heating at 300 °C, 450 °C and 600 °C, (a) saturated flint, (b) dry flint.

aggregate is obtained by performing a mean, weighed according to the proportion of the different petrographic types of the aggregates. Fig. 5 shows the evolution of the porosity of C, SC and S aggregates as a function of heating temperature.

The porosity of flints could not be measured after 150 °C because the flints broke into multiple fragments hardly retrievable in the oven. For SC aggregates, the porosity study was then only carried out on carbonates. Fig. 5 shows that flint aggregates have a very low porosity, less than 1%. The carbonates from SC aggregates are more porous than those from C aggregates. Porosities of the C and S aggregates are similar and do not vary up to 300 °C. Beyond 300 °C, the porosity of the carbonates increases more significantly.
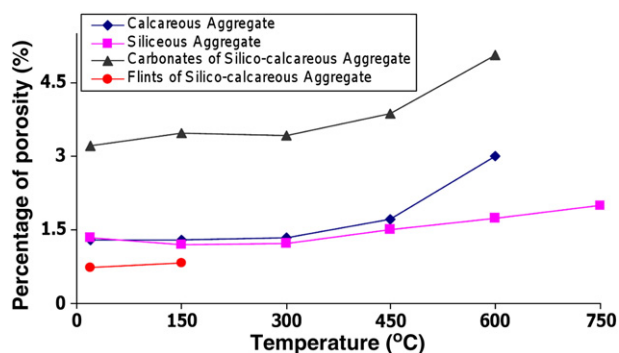

Fig. 5. Evolution of the porosity of calcareous, silico-calcareous, and siliceous aggregates after heating–cooling cycles.

3.1.3. Aggregate mass loss

The mass loss value is obtained by an average made on 8 grains for every mineralogical type of aggregates. Mass loss values and standard deviation for SC aggregates, S aggregates and C aggregates are listed in Table 3.

As the saturated flints have exploded at the heating cycle at 300 °C, mass loss measurements were made only on oven-dry flints. According to Table 3, mass loss of oven-dry flints was nearly stable up to 450 °C. Over 450 °C, mass loss of dry flints increases significantly about 1% on the non-spalled sample.

The mass loss of saturated aggregates between 0 and 150 °C corresponds to the departure of absorbed water. Carbonates of the SC aggregates are more porous than other aggregates and have consequently higher weight loss between 0 and 150 °C. After stabilisation between 150 °C and 300 °C, carbonates show another mass loss after the 450 °C cycle, 3.01% for carbonates from SC aggregates and 0.63% for carbonates from C aggregates. Between 600 and 750 °C, the mass loss accelerates, reaching approximately 10% for both types of carbonate.

The mass loss of the quartzites (S aggregates) is very low, in the order of a thousandth. This value is of the same order of magnitude as results reported in Homand's works [42].

This study has pointed out the different behaviours of the studied aggregates with the rise of temperature. Decarbonation of carbonates was clearly observable after heating at 750 °C. However modification of carbonate physical characteristics such as the increase of porosity and mass loss starts between 450 °C and 600 °C. Regarding aggregates of siliceous nature, flints (SC aggregates) show an important thermal instability whereas for quartzite aggregates (S aggregates) only a low or slight increase of porosity occurs after 300 °C. The mass loss observed in flints after 450 °C may be related to the departure of trapped water as well as structural hydroxyl water of silanol ($SiO_{5/2}$ H) groups.

Table 3
Average mass loss and standard deviation values for SC-aggregates, S-aggregates and C-aggregates. (* : samples not exploded).

	150 °C		300 °C		450 °C		600 °C		750 °C	
	Average mass loss	Standard deviation	Average mass loss	Standard deviation	Average mass loss	Standard deviation	Average mass loss	Standard deviation	Average mass loss	Standard deviation
Saturated flints in SC aggregates	0.472%	0.392	Spalling	Spalling	Spalling	Spalling	Spalling	Spalling	Spalling	Spalling
Oven-dry flints in SC aggregates	0.004%	0	0.061%	0	0.156%	0	1.029%*	0.009*	Spalling	spalling
Saturated carbonates in SC aggregates	5.253%	2.703	5.300%	2.220	5.486%	1.875	8.500%	4.238	18.977%	5.844
Saturated S Aggregates	0.404%	0.2159	0.462%	0.154	0.520%	0.318	0.568%	0.218	0.557%	0.346
Saturated C aggregates	0.492%	0.188	0.712%	0.239	0.761%	0.207	1.387%	0.799	10.940%	1.336

3.2. Evolution of physical properties of concrete composed of various aggregates

3.2.1. Description of thermal damage of concretes

For all concretes, the first cracks are observed after the heating/cooling cycle at 300 °C. The highest rate of cracking is observed for SC concrete. Fig. 6 shows cracking and surface spalling affecting high performance and ordinary SC concrete specimens after heating at 600 °C and 750 °C.

Explosive spalling occurred on some specimens of high-performance concrete made of S aggregates (in the proportion of 1/7) and SC aggregates (in the proportion of 2/9) at 600 °C and 750 °C. C aggregate concretes heated at 750 °C are disintegrated several days after cooling due to the hydration of CaO in $Ca(OH)_2$ in the mortar and in the aggregates. The formation of portlandite is associated to a volume increase and leads to specimen disintegration. The same phenomena are also observed on NC-SC, NC-S, HPC-SC and HPC-S after the heating/cooling cycle at 750 °C. But they are much slower and less intense than on concrete with C aggregates.

3.2.2. Study of cracking

In order to compare and analyse the cracking evolution in the different types of concrete, Ø16×32 cm concrete specimens were sawn in Ø16×5 cm slices and were submitted to heating–cooling cycles. Image analysis is used for mapping the cracks and measuring the width and the area of cracks. The density of cracks is quantified by the area of cracks in total surface of concrete disk. After heating at 300 °C, only few microcracks can be observed using optical microscopy. Fracturation of ordinary concretes after heating–cooling cycle at 600 °C is reported in Fig. 7.

At 600 °C, the concrete with flint aggregates is more damaged than the concrete with calcareous aggregates and quartzite aggregates. This observation was also reported by Hager [14]. For SC concrete, the cracks are joined forming a network distributed over the entire surface of the sample. The crack area is about 5.44% of the surface of concrete specimen. The maximum crack width is about 600 μm. Cracks are mainly located at the paste–aggregate interface but can also pass through the aggregates.

For S concrete, cracks are less dense, mainly located in the periphery of the sample. The crack area is about 1.56% of the surface of concrete specimen. Cracks are observed at the paste–aggregate interface and in the paste. The maximum crack width is about 300 μm.

For C concrete, cracks are isolated and do not form a network. The crack area is about 1% of the surface of concrete specimen and the maximum crack width is about 80 μm.

3.2.3. Thermal conductivity

Thermal conductivity and standard deviation values are given in Table 4 for the studied concretes. Standard deviations on these measurements are less than 10%, except for the heating–cooling cycle at 750 °C. At this temperature the significant cracking of the concrete makes the sample highly heterogeneous which explains the higher standard deviation. Thermal conductivity values are plotted with error bars representing the standard deviations to assess the significance of the results (Fig. 8a and c).

At 20 °C, Table 4 shows that the concrete with quartzite aggregates (siliceous) has a higher thermal conductivity (3.13 W/m°C for NC and 3.33 W/m°C for HPC) than concrete with C aggregates (1.63 W/m°C for NC and 1.85 W/m°C for HPC) and concrete with SC aggregates
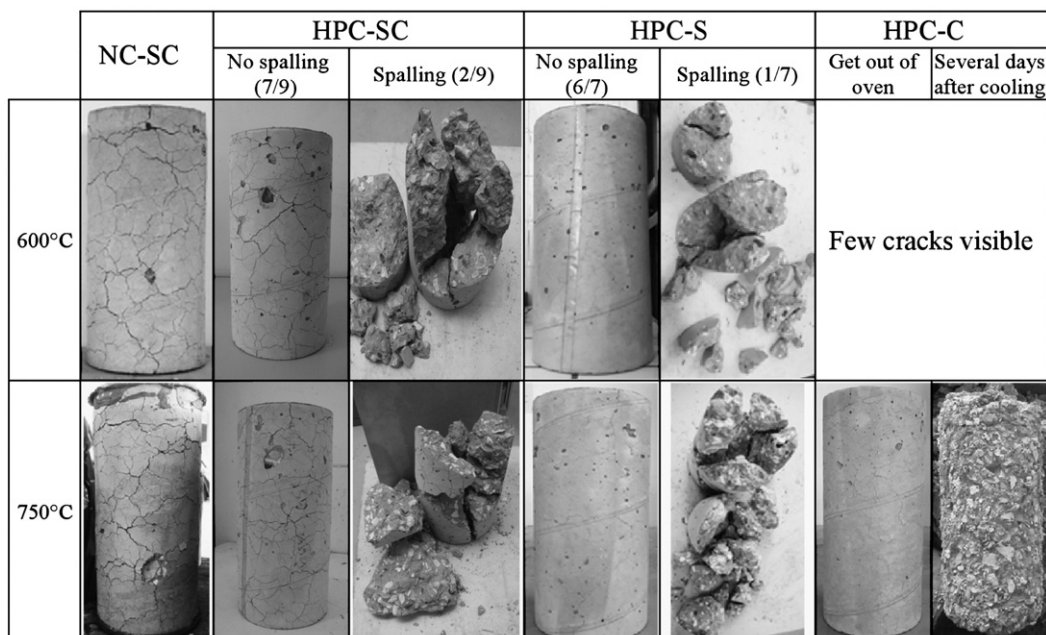
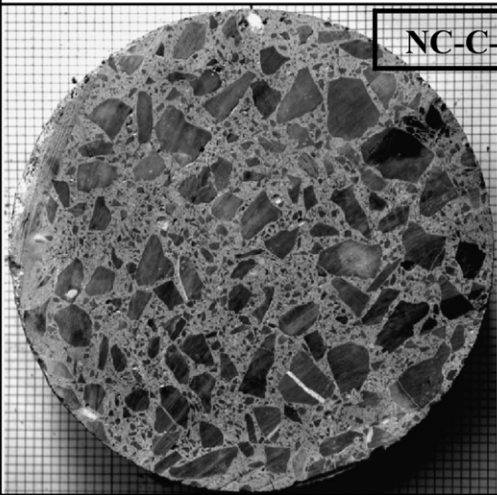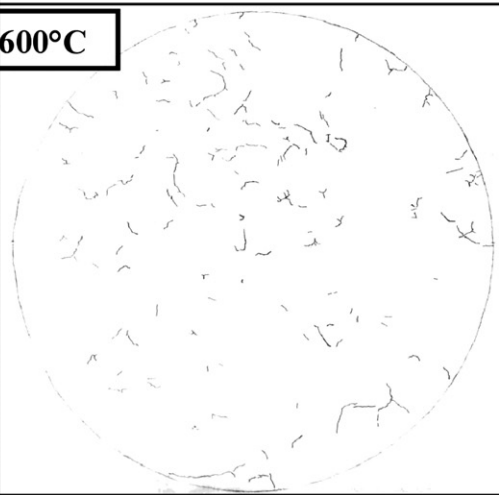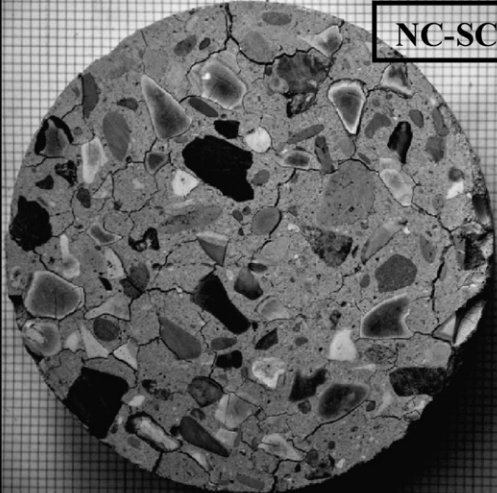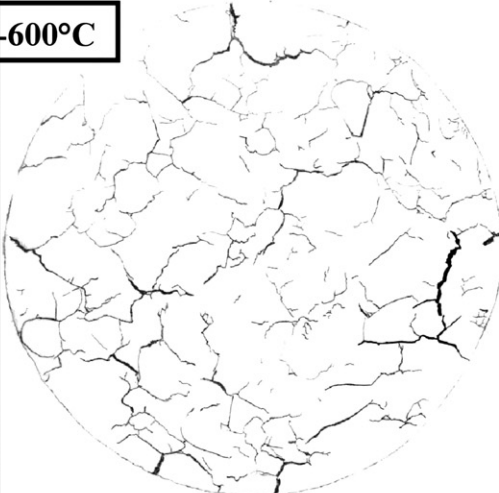**Fig. 6.** Specimens Ø16×32 after heating/cooling cycles at 600 °C and 750 °C.
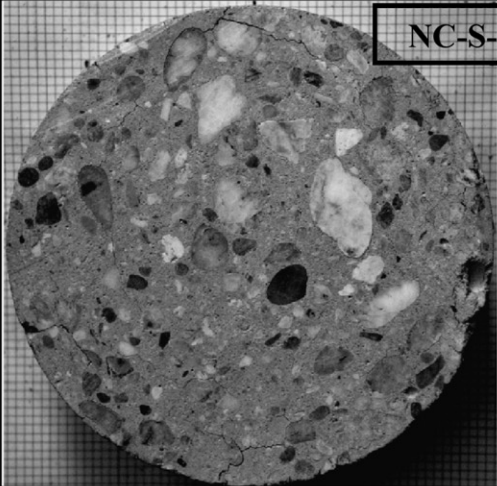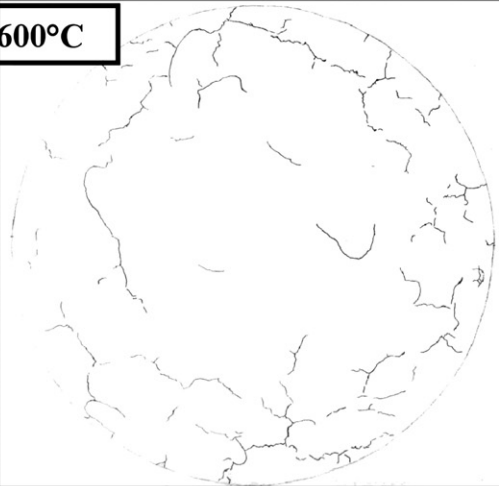
Photographe after heating	Cracking map	Percentage of cracks area
NC-C-600°C		0,99%
NC-SC-600°C		5,44%
NC-S-600°C		1,56%

Fig. 7. Comparison of the fracturation of NC-S, NC-C and NC-SC after heating/cooling cycle at 600 °C.

(1.86 W/m°C for NC and 2.06 W/m°C for HPC). These results are explained by the higher thermal conductivity of quartz (7.7 W/m°C) compared to that of calcite (2 to 3 W/m°C) [43]. Moreover SC aggregates contain 70% of siliceous aggregates (flints), but thermal conductivity of concrete with SC aggregates is close to that of concrete with C aggregates, because quartz in flint is cryptocrystalline, and has consequently a lower thermal conductivity than macrocrystalline quartz into quartzite.

Thermal conductivity was measured after cooling to room temperature. Fig. 8 shows that the thermal conductivity decreases when the heating temperature increases. This is linked to the deterioration of the microstructure. The voids limit the heat transfer.

Table 4
Average thermal conductivity and standard deviation values of the studied concretes after heating.

		20 °C			300 °C			600 °C			750 °C		
		Average thermal conductivity	Standard deviation	Average	Average thermal conductivity	Standard deviation	Average	Average thermal conductivity	Standard deviation	Average	Average thermal conductivity	Standard deviation	Average
NC	SC	1.86	4.3%	4.7%	1.78	5.6%	5.5%	0.99	7.1%	8.0%	0.70	24.3%	18.6%
	S	3.13	3.2%		2.66	2.6%		1.25	10.0%		1.21	12.4%	
	C	1.63	6.7%		1.54	8.4%		1.01	6.9%		0.84	19.0%	
HPC	SC	2.06	8.7%	6.5%	1.98	5.5%	5.4%	1.18	8.5%	7.2%	1.16	23.3%	14.5%
	S	3.33	4.2%		2.88	5.9%		2.06	8.7%		1.60	11.3%	
	C	1.85	6.5%		1.68	4.8%		1.16	4.3%		1.12	8.9%	

Indeed, the loss of conductivity is higher for normal concretes (50%) than for high performance concretes (40%).

With the increase of temperature, the difference of thermal conductivity among the concrete with quartzite, calcareous or flint aggregates becomes smaller. The thermal conductivity of concrete with quartzite aggregates declines more rapidly than that of concretes with flint (SC) or calcareous (C) aggregates (Fig. 8b and d). As shown by the study of the cracking, this cannot be explained by a greater damage of concretes with quartzite aggregates. The temperature dependence of the thermal conductivity is related to the mineral crystallinity. The thermal conductivity decreases more with the rise of temperature for well-crystallised structure than for poorly-crystallised structure [44]. The relative loss of thermal conductivity is lower for high-performance concretes than for normal concretes. The improvement provided by the high-performance matrix varies with the aggregate type. It is more important for S and SC concretes than for C concretes. Thus there are lower differences of relative loss of thermal conductivity between the different HP concretes than between the normal concretes.

The decrease in thermal conductivity after heating can be explained by cracking at the paste–aggregate interface and in the paste, by the dehydration of the paste and by the fracture of intercrystalline link in the aggregate because of an excessive thermal expansion [45].

3.2.4. Concrete mass loss

The mass loss value is an average of measurements carried out on 4 specimens (Ø16 × 32 cm) for each type of concrete. The average value and standard deviation of the mass loss for SC concretes, S concretes, and C concretes are listed in Table 5.

For a given matrix (normal or high performance) the paste volume is kept unchanged for the three natures of aggregates (S, SC and C). So difference in mass loss between concretes is only linked to the nature of aggregates.

For a W/C ratio of 0.6, the mass loss of different concretes is very similar up to 300 °C. Beyond this temperature, the mineralogical nature of aggregates influences the mass loss of concretes (Fig. 9). For a W/C ratio of 0.3, differences between mass loss already appear at
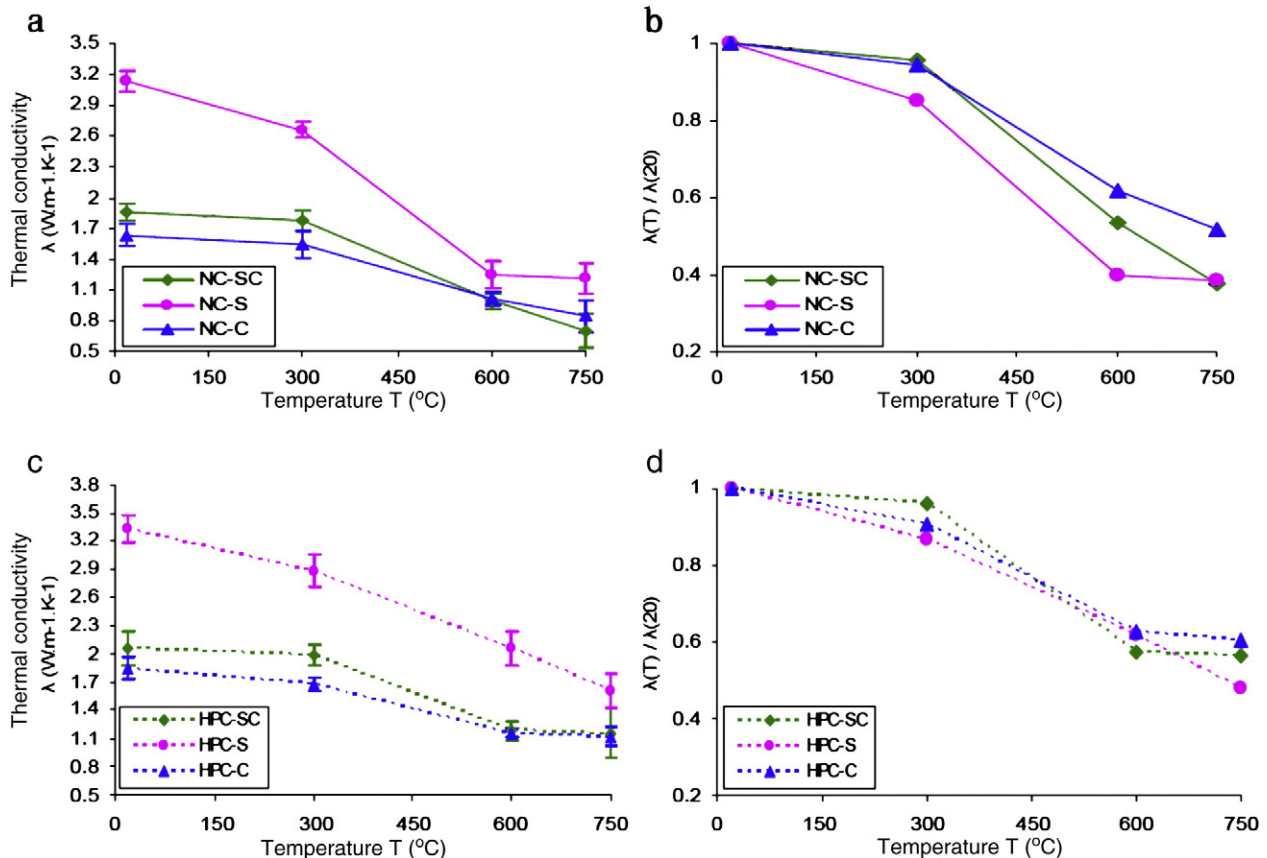
Fig. 8. Evolution of the thermal conductivity of concretes after heating/cooling cycles, (a) absolute values of normal concretes, (b) relative values of normal concretes, (c) absolute values of high-performance concretes, (d) relative values of high-performance concretes.

Table 5
Average mass loss and standard deviation values of studied concretes after heating.

		300 °C		600 °C		750 °C	
		Average mass loss	Standard deviation	Average mass loss	Standard deviation	Average mass loss	Standard deviation
NC	SC	6.2%	0.025	9.5%	0.027	9.9%	0.079
	S	5.9%	0.192	7.8%	0.239	7.7%	0.130
	C	6.6%	0.122	8.8%	0.094	10.3%	0.317
HPC	SC	4.9%	0.098	7.1%	0.051	7.5%	0.017
	S	3.0%	0.158	5.3%	0.014	5.7%	0.010
	C	4.1%	0.136	6.1%	0.117	7.4%	0.143

300 °C (Fig. 9). For HP concretes, on the total amount of free water into the concrete, the importance of the part contained in the paste decreases relative to the part contained in aggregates. So, at 300 °C the differences in mass loss between the three high-performance concretes can be explained by the free water brought by aggregates. The amounts of concrete mass loss are in accordance with the results of the aggregate's mass loss. Concretes with quartzite aggregates (S) have the lowest weight loss according to the results obtained on aggregates only. These results corroborate those reported by Mindéguia [29] who found that the mass of silico-calcareous concretes decreases more rapidly than calcareous concretes. Silico-calcareous aggregates of our study are similar to those of Mindeguia's works. The greater mass loss of silico-calcareous concretes can be explained partly by the important absorbed water of the porous carbonates (Table 3) and the departure of bound water from the flints [46].

Moreover, the mass loss of concretes with SC aggregates and with S aggregates stabilises from 600 °C. In reverse, the CO_2 gas release from calcium carbonates might explain the weight loss after 600 °C for concretes with calcareous aggregates.

3.3. Residual mechanical properties

3.3.1. Normal concretes

At 20 °C, concretes with SC, C and S aggregates have very similar mechanical characteristics (Table 2). After heating and cooling, the residual mechanical properties of NC-C are higher than those of NC-S and NC-SC. At 600 °C, NC-SC shows a loss in performance higher than 90% (Fig. 10a).

The evolution of residual compressive strength is similar for the three concretes up to 300 °C. In fact, most of the damage at this step comes from the elimination of free water and from the dehydration of CSH in concrete. Beyond, the aggregate nature affects the degradation of the concrete, the strength loss becoming more important for the NC-SC. This observation is noted also by Marechal [47]. The use of C aggregates increases the residual compressive strength to about 50% at 600 °C compared with SC aggregates and the use of quartzite aggregates increases the residual compressive strength to about 35%
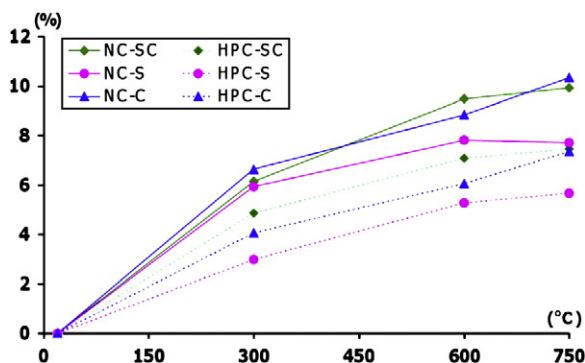

Fig. 9. Mass loss of the tested concretes as a function of the heating temperature.

at 600 °C compared with SC aggregates. The strength of NC-C decreases slightly compared to that of NC-SC and NC-S between 300 °C and 600 °C. Abrams has also reported this observation [21]. This result is partially adapted to that predicted in Eurocode [12]. However, over 600 °C, the strength loss of NC-C and NC-S continues contrary to the NC-SC and the improvement decreases from 32 to 21% for NC-S and from 47% to 20% for NC-C. Mechanical tests were performed immediately after the cooling. The residual performances after heating at 750 °C would have been lower for C concretes if the specimens would have been tested several hours after. Indeed, the hydration of CaO in $Ca(OH)_2$ is associated to a volume increase and leads to specimen disintegration.

As for residual tensile strength and residual Young's modulus, the behaviour of NC-C is significantly better than that of NC-SC and of NC-S after heating at 600 °C. The C concrete has the best residual tensile strength. After heating at 600 °C, its residual strength is 56.3% of the original strength instead of 20% and 10.8% for NC-S and NC-SC respectively. The loss of tensile strength of NC-S concrete is higher than its loss of compressive strength. It can be explained by microcracking at the paste–aggregate interface. The better performance of NC-C compared to NC-S in tension is probably due to better bonding of C aggregates to the paste. Quartzite aggregates are round and have a smooth surface conversely to C aggregates which are crushed and have a rough texture. In addition, there are chemical reactions between C aggregates and the paste which improve adhesion strength. Beyond 600 °C, the loss of tensile strength of NC-C becomes more important because of the dissociation of calcium carbonate.

The residual Young's modulus of normal concretes after exposure to high temperatures shows the same observations. The ascending order of residual performances is NC-SC, NC-S and NC-C. The differences between the three concretes are less significant than for compressive or tensile strength.

The differences in residual mechanical performances are particularly important between 300 and 600 °C. The paste mechanical properties and volume are the same for all three concretes and the differences in residual mechanical performance are related to differences in mineralogical and chemical composition of aggregates. Due to decarbonation, mechanical strength of C aggregates decreases after 600 °C. For the same chemical nature (Siliceous) the quartzite aggregates show greater thermal stability than the flint aggregates.

3.3.2. High performance concretes

Fig. 10b shows the evolution of residual mechanical characteristics of high-performance concretes made with SC aggregates, S aggregates and C aggregates.

In terms of compressive strength, the HPC-S has better residual behaviour than the HPC-SC and the HPC-C. This result disagrees with the Eurocode predictions [12] but F. Robert has reported a similar trend [11]. She has shown that two of three tested concretes with siliceous aggregates have better results than concrete with calcareous aggregates. The strength loss difference between HPC-S and HPC-C is 18% at 600 °C and 20% at 750 °C. The strength loss difference between HPC-S and HPC-SC is 65% at 600 °C and 42% at 750 °C. The residual strength of HPC-C is much higher than that of HPC-SC at 600 °C in our study. This observation is consistent with previous studies of other researchers [29,48] for a given high performance matrix. In comparison to normal concretes, the loss of compressive strength of HPC-S is moderate up to 600 °C and accelerates beyond this temperature. The better compressive and tensile behaviour of HPC-S compared with NC-S can be explained by higher bond strength at the paste–aggregate interface. The lower water-to-cement ratio of the paste leads to a decrease of the porosity of the interfacial transition zone. It can be noted that the increase of quartzite aggregates volume due to quartz α to quartz β transformation which occurs at 573 °C does not lead to poorer performances of S concretes over C concretes. The compressive strength loss of high performance concrete with SC aggregates between 300 and 600 °C is due to spalling of flints.
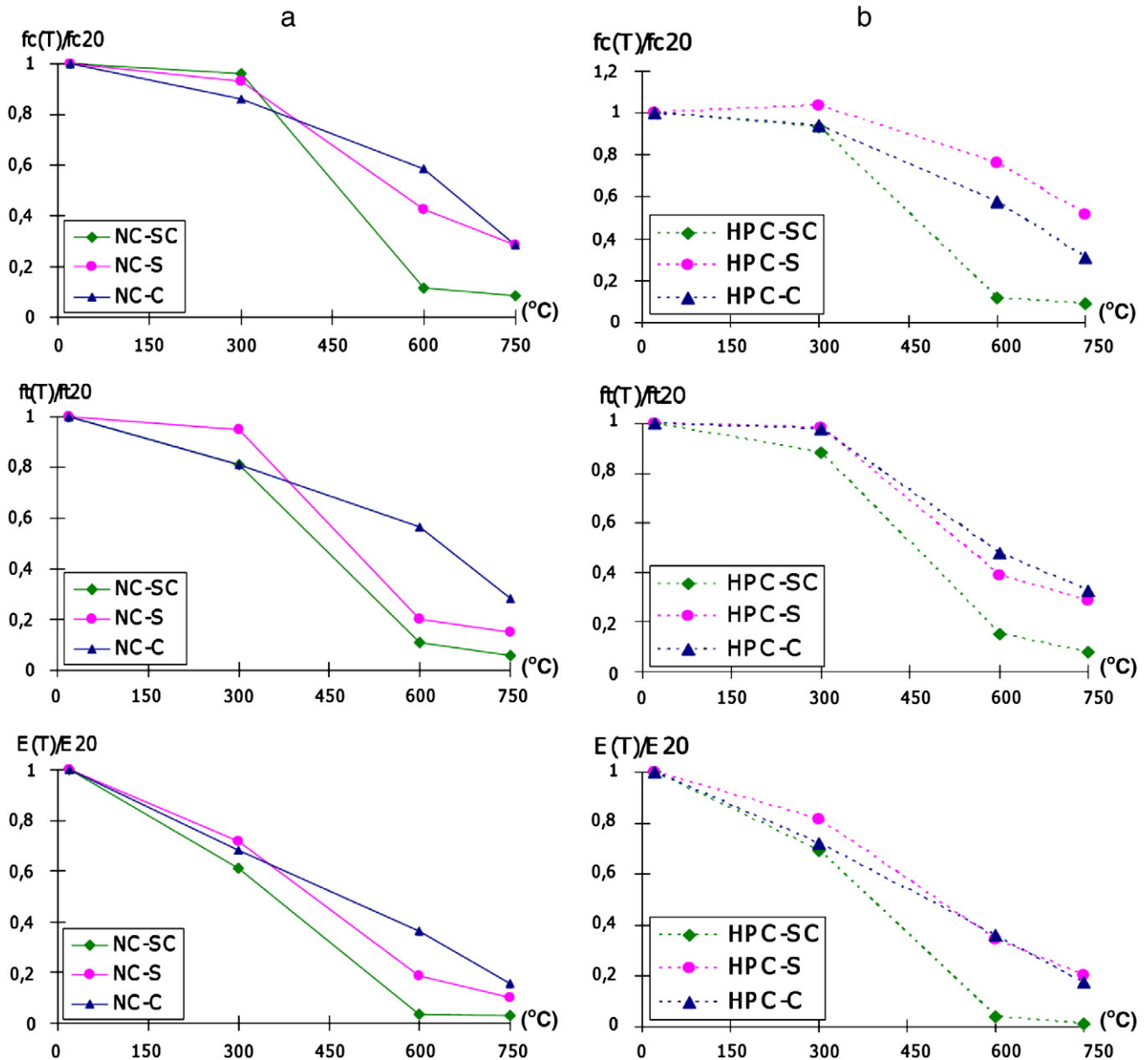
a

b

Fig. 10. The residual mechanical performances of concretes as a function of heating temperature, (a) normal concretes. (b) high-performance concretes.

In terms of tensile strength, C concretes degrade less than S concrete. Reduction in Young's modulus is almost the same for C concrete and S concrete. Like for normal concretes, the residual mechanical properties of concretes with SC aggregates (flints) are much lower compared with HPC-S and HPC-C.

4. Conclusion

This article presents a comparative analysis of mechanical and physical properties of six concretes exposed to heating/cooling cycles at 300 °C, 600 °C and 750 °C at a heating rate of 1 °C/min. To analyse the influence of the nature of aggregates, our research work was divided into two parts: in the first part the evolution of physical properties of aggregates itself after heating–cooling cycle was investigated and in the second part the residual mechanical behaviour, the evolution of cracking, of mass loss and of thermal conductivity of concretes composed of the previous aggregates was studied. Two types of paste matrix were tested, normal and high performance ones.

The study of the thermal behaviour of aggregates showed the importance of the initial moisture state for the flint aggregates. Explosive spalling occurred between 150 °C and 450 °C for saturated ones. The low porosity of flint aggregates leads to a build-up of vapour pressure as a result of a bad drainage pore volume. The permeability of aggregates plays an important role in the thermal stability. With a similar siliceous nature, quartzite and flints have a completely different behaviour; oven-dry flint aggregates showed important damages after 450 °C (cracks, bursting into fragments) while quartzite aggregates present the lowest values of mass loss and of porosity increase among the three tested aggregates. The crystallisation and microstructure of quartz seem to play an important role in the thermal stability of siliceous aggregates.

Concretes with the same paste volume and composition were made with the three different types of aggregates. The residual mechanical behaviour varies depending on the aggregates. The SC concrete presents severe cracking, and significant mechanical strength loss between 300 and 600 °C. For example, residual compressive strength of NC-SC concrete at 600 °C is 4.2 MPa which is 3–5 times lower than that of NC-S concretes and NC-C concretes respectively. The thermal instability of flints contained

into SC aggregates explains the higher damage of SC-concretes with the temperature increase. For C-concrete, lime coming from the decarbonation of calcite (between 600 °C and 750 °C) reacts with ambient humidity and forms Portlandite by multiplying its volume by 2.5. This increase of volume leads to concrete disintegration. The residual mechanical characteristics must be measured shortly after the cooling. Values after the heating at 750 °C would be lower for C-concrete several hours after the cooling.

The influence of the aggregates is also dependent on the paste composition; with normal matrix C-concrete has the best residual compressive strength while with a high-strength matrix the S-concrete behaves the best. With a lower W/C ratio, the porosity of the paste–aggregate interface zone decreases, and bond strength between paste and aggregate is improved. The increase of quartzite aggregate volume due to quartz α to quartz β transformation which occurs at 573 °C causes cracking at the paste–aggregate interface. A better tensile strength at the interface delays the occurrence of cracks.

Acknowledgments

References

[1] P. Kalifa, F.D. Menneteau, D. Quenard, Spalling and pore pressure in HPC at high temperatures, Cement and Concrete Research 30 (2000) 1915–1927.
[2] T. Chaussadent, V. Baroghel-Bouny, N. Rafaï, A. Ammouche, H. Hornain, Influence du rapport E/C sur l'hydratation, la microstructure et les déformations endogènes de pâte de ciment durcies, Revue Française de Génie Civil 5 (2001) 217–230.
[3] B. Georgali, P.E. Tsakiridis, Microstructure of fire-damaged concrete—a case study, Cement and Concrete Composites 27 (2005) 255–259.
[4] M. Kanema, M.V.G. De Morais, A. Noumowe, J.L. Gallias, R. Cabrillac, Experimental and numerical studies of thermo-hydrous transfers in concrete exposed to high temperature, Heat and Mass Transfer 44 (2007) 149–164.
[5] J.C. Maso, La liaison pâte-granulats, in: J. Baron, R. Sauterey (Eds.), Le Béton Hydraulique, Presse de l'ENPC, Paris, 1982, pp. 247–259.
[6] F. De Larrard, Construire en Béton-L'essentiel sur les Matériaux, Presse de l'ENPC, Paris, 2002.
[7] R. Felicetti, P.G. Gambarova, The effects of high temperature on the residual compressive strength of high-strenght siliceous concretes, ACI Materials Journal 95 (1998) 395–406.
[8] V.R. Kodur, M.A. Sultan, Structural Behaviour of High Strength Concrete Columns Exposed to Fire, International Symposium on High Performance and Reactive Powder Concrete, Sherbrooke, 1998, pp. 217–232.
[9] A. Savva, P. Manita, K.K. Sideris, Influence of elevated temperatures on the mechanical properties of blended cement concretes prepared with limestone and siliceous aggregates, Cement and Concrete Composites 27 (2005) 239–248.
[10] G.A. Khoury, Y. Anderberg, K. Both, J. Fellinger, N.P. Hoj, C. Majorana, Fire design of concrete structures-materials, structures and modelling, State-of-art report, Fib Bulletin, 38, 2007.
[11] F. Robert, H. Colina, The influence of aggregates on the mechanical characteristics of concrete exposed to fire, Magazine of Concrete Research 61 (2009) 311–321.
[12] European Committee for Standardization, EN 1992-1.2, Eurocode 2 Design of Concrete Structures, CEN, Brussels, 2004.
[13] Properties of materials at high temperatures — concrete, in: Schneider (Ed.), RILEM TC 44-PHT, 1985.
[14] I. Gaweska Hager, Comportement à haute température des bétons à haute performance-évolution des principales propriétés mécaniques, Thèse de ENPC, 2004.
[15] D. Matesova, D. Bonen, S.P. Shah, Factors affecting the resistance of cementitious materials at high temperatures and medium [0] heating rates, Materials and Structures 39 (2006) 455–469.
[16] V. Kodur, R. Mcgrath, Fire endurance of high strength concrete columns, Fire Technology 39 (2003) 73–87.
[17] ASTM STP 169D, Significance of tests and properties of concrete and concrete-making materials, in: J.F. Lamond, J.H. Pielert (Eds.), ASTM International, 2006, 645 pp.
[18] E. Annerel, L. Taerwe, Revealing the temperature history in concrete after fire exposure by microscopic analysis, Cement and Concrete Research 39 (2009) 1239–1249.
[19] A. Noumowé, P. Clastres, G. Debicki, J.-L. Costaz, Transient heating effect on high strength concrete, Nuclear Engineering and Design 166 (1996) 99–108.
[20] T. Harada, J. Takeda, S. Yamane, F. Furumura, Strength, elasticity and thermal properties of concrete subjected to elevated temperatures, Concrete for nuclear reactors, ACI Special Publication, 34, 1970, pp. 377–406, Detroit.
[21] M. Abrams, Compressive strength of concrete at temperature to 1600 F, Temperature and concrete, ACI Special Publication, 25, 1971, pp. 33–58, Detroit.
[22] G. Sanjayan, L. Stocks, Spalling of high-strength silica fume concrete in fire, ACI Materials Journal 90 (1993) 170–173.
[23] R. Felicetti, P.G. Gambarova, M. Semiglia, Residual capacity of HSC thermally damaged deep beams, Journal of Structural Engineering 125 (1999) 319–327.
[24] I. Hager, P. Pimienta, Mechnical properties of HPC at high temperature, Fib task group 4.3 "Fire design of concrete structures", 2–4 December 2004, Milan.
[25] R. Dupain, R. Lanchon, J.-C. Saint-Arroman, Granulats, Sols, Ciments et Bétons, Caractérisation des matériaux de génie civil par les essais de laboratoire, 2nd ed. Casteilla, Paris, 2000.
[26] Rilem Technical, Committees 129-MHT, Test methods for mechanical properties of concrete at high temperatures, part 1: introduction, part 2: stress–strain relation, part 3: compressive strength for service and accident conditions, Materials and Structures 28 (1995) 410–414.
[27] S.E. Gustafsson, T. Log, Transient plane source (TPS) technique for measuring thermal transport properties of building materials, Fire and Materials 19 (1995) 43–49.
[28] Y. He, Rapid thermal conductivity measurement with a hot disk sensor-part 1: theoretical considerations, Thermochimica Acta 436 (2005) 122–129.
[29] J.-C. Mindeguia, Contribution expérimentale à la compréhension des risques d'instabilité thermique des bétons, Thèse de doctorat de l'Université de Pau et des Pays de l'Adour, 2009.
[30] J.M. Torrenti, P. Dentec, C. Boulay, J.F. Sembla, Projet de processus d'essai pour la détermination du module de déformation longitudinale du béton, Bulletin des Laboratoires des Ponts et Chaussées 220 (1999) 79–81.
[31] E. Rayssac, J.C. Auriol, D. deneele, F. Larrard, V. Ledee, G. Platret, Valorisation de laitiers d'aciérie LD pour les infrastructures routières, Bulletin des Laboratoires des Ponts et Chaussées 275 (2009) 27–38.
[32] J.-C. Mindeguia, P. Pimienta, A. Noumowé, M. Kanema, Temperature, pore pressure and mass variation of concrete subjected to high temperature, Cement and Concrete Research 40 (2010) 477–487.
[33] C. Meyer-Ottens, The question of spalling of concrete structural elements under fire loading, PhD Thesis, Technical University of Braunschweig, Germany, 1972.
[34] G.A. Khoury, Effect of heat on concrete material, Imperial college report, 1995, p. 73.
[35] E.F. Vansant, P. Van Der Voort, K.C. Vrancken, Characterization and Chemical Modification of the Silica Surface, Elsevier, Amsterdam, 1995.
[36] W.A. Deer, R.A. Howie, J. Zussman, An Introduction to the Rock Forming Minerals, 2nd ed. Longman Scientific & Technical, New York, 1992.
[37] L.T. Zhuravlev, Structurally bound water and surface characterization of amorphous silica, Pure and Applied Chemistry 61 (1989) 1969–1976.
[38] S. Ek, Determination of the hydroxyl group content in silica by thermogravimetry and a comparison with 1 H MAS NMR results, Thermochimica Acta 379 (2001) 201–212.
[39] M. Domanski, J. Webb, R. Glaisher, J. Gurba, J. Libera, A. Zakościelna, Heat treatment of Polish flints, Journal of Archaeological Science 36 (2009) 1400–1408.
[40] B.A. Purdy, Investigations concerning the thermal alteration of silica materials: an archaeological approach, Tebiwa 17 (1974) 37–66.
[41] L.W. Patterson, Thermal damage of chert, Lithic Technology 20 (1995) 72–80.
[42] F. Homand-Etienne, Comportement mécanique des roches en fonction de la température, Thèse de doctorat d'Etat des Sciences, INPL, Nancy, Mémoire Sciences de La Terre n° 46, 1986, 261 pp.
[43] Comité Français de Mécanique des Roches, Manuel de mécanique des roches, Tome 1, Presses Ecole des Mines, Paris, 2000.
[44] J.P. Mercier, G. Zambelli, W. Kurz, Introduction à la Science des Matériaux, third ed. Presses Polytechniques et Universitaires Romandes, Lausanne, 1999.
[45] J. Lamond, J. Pielert, Significance of Tests and Properties of Concrete and Concrete-making Material, ASTM International, West Conshohocken, 2006.
[46] J. Verstraete, Approche multi-technique et multi-échelle d'étude des propriétés structurales des matériaux hétérogènes: application à un granulat siliceux naturel, Thèse de doctorat de l'Université de Mulhouse, 2005.
[47] J.C. Marechal, Contribution à l'étude des propriétés thermiques et mécaniques du béton en fonction de la température, Annales de l'Institut Technique et du BTP 274 (1970) 121–146.
[48] Irex, Synthèse des Travaux du Projet National BHP 2000 sur les Bétons à Haute Température, Presses de l'école nationale des ponts et chaussées, 2005.